

Long-Lived Multifunctional Superhydrophobic Heterostructure Via Molecular Self-Supply

Yongfeng Huang, Ying Hu, Chongqin Zhu, Fan Zhang, Hui Li, Xinghua Lu, and Sheng Meng*

Superhydrophobic (SHO) surfaces have drawn great attention thanks to their theoretical significance and myriad applications in industry and everyday life. Current approaches to fabricate such surfaces require calcinating at high temperatures, tedious and time-consuming treatments, toxic chemicals, and/or processing with intricate instruments. Long-duration SHO surfaces are even more challenging due to material instability and easy contamination by organic pollutants in dry conditions. To overcome these difficulties we design a simple approach via self-supplying of low surface tension chemicals to nanoparticles to fabricate multifunctional SHO heterostructures. The method herein features room temperature, rapid processing, with environment-friendly raw materials. With multiple functions such as photocatalysis and transparency SHO surfaces further extend their lifetime and enable self-sustaining environment maintenance.

1. Introduction

A surface is considered to be superhydrophobic (SHO) when water droplets form a contact angle (CA) larger than 150° upon adsorption and slide down at a tilted angle lower than 10° .^[1] Such a surface exhibits both theoretical importance and practical applicability in areas including biology, long-range interaction, heat transfer, transportation, tribology, and microfluidics.^[2–7] One example is self-cleaning of dirt and pollutants from surfaces in environmental maintaining and microfabrication.^[8] Maintaining SHO properties for a long lifetime is a major challenge, since SHO surfaces are easily contaminated by organic pollutants and stop functioning in practice. As a result, SHO materials with lifetime longer than a year are rarely reported.^[9–12] Low cost, high efficiency fabrication of long-lived SHO surfaces is therefore crucial for large-scale applications.

Although noteworthy progresses on microscopic mechanisms have been achieved,^[13–16] fabrication of SHO surfaces

encounters many difficulties. Mimicking the lotus effect of plant leaves, SHO surfaces were found to be resulted from surface microstructures together with hydrophobic chemicals. Surface microstructures can be fabricated by various means including chemical vapor deposition (CVD), ion-beam and e-beam lithography.^[17–22] However, these methods suffer from disadvantages such as calcinating at high temperatures, tedious and time-consuming treatments, toxic chemicals, or processing with intricate instruments. For instance, Lau et al. deposited carbon nanotube forests on oxidized silicon by CVD at 650°C with DC voltage bias of 600 V and then coated the forests with poly(tetrafluoroethylene) to achieve SHO

surfaces.^[17] Deng et al. coated candle soot with silica at 600°C for 24 h to fabricate superamphiphobic coatings.^[18] Operating at temperatures $\geq 600^\circ\text{C}$ this approach is highly energy-intensive; it is also time-consuming costing days or longer. Lithography based on ion-beam and e-beam is also widely employed to fabricate microstructural surfaces.^[19,20] However, this approach heavily relies on intricate ion-beam and e-beam instruments which are not easily accessible. Other problems include toxicity and instability of raw materials applied. Hydrophobic chemicals and organic polymers such as perfluorosilane, octadecyltrichlorosilane, tetraethylorthosilicate, and others are commonly used to coat surface microstructures.^[20–22] However, these chemicals are toxic, combustible, nonresistant to sunlight, unstable at high temperature ($>260^\circ\text{C}$), and/or difficult to maintain.

Here we report a simple approach, based on self-supplying of low surface tension chemicals to nanoparticles, to fabricate SHO heterostructural surfaces featuring low temperature, rapid processing, with simple instruments and environment-friendly materials. Long-duration outdoor superhydrophobicity maintained for over a year is achieved. Furthermore, the surfaces made are endowed with extraordinary functions such as photocatalysis and transparency, enabling self-sustaining dust removal, and organic decomposition without poisoning. Besides, the heterostructures can be mounted flexibly into ultrafine wettability patterns favoring water collection and microfluidic applications.

2. Results and Discussion

The SHO surface in our experiment is a three-layer heterostructure, which can be fabricated on different types of substrates

Y. Huang, Y. Hu, C. Zhu, F. Zhang, Dr. H. Li,
Prof. X. Lu, Prof. S. Meng
Beijing National Laboratory for Condensed
Matter Physics and Institute of Physics
Chinese Academy of Sciences
Beijing 100190, China
E-mail: smeng@iphy.ac.cn

Y. Huang, Y. Hu, C. Zhu, F. Zhang, Dr. H. Li,
Prof. X. Lu, Prof. S. Meng
Collaborative Innovation Center of Quantum Matter
Beijing 100190, China



DOI: 10.1002/admi.201500727

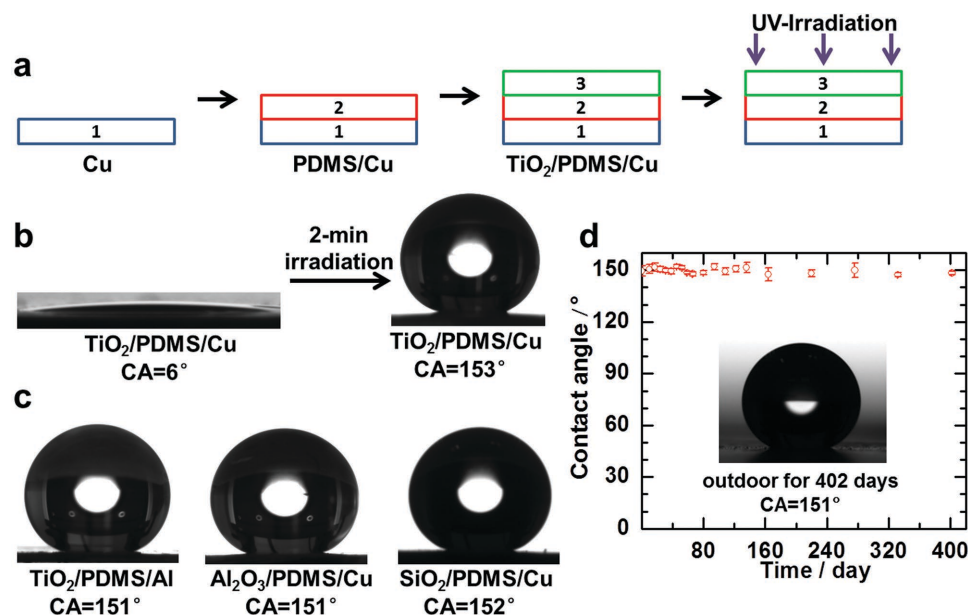


Figure 1. Fabrication procedure of a superhydrophobic $\text{TiO}_2/\text{PDMS}/\text{Cu}$ heterostructure and its versatility and durability. a) The schematic showing fabrication procedure of the heterostructure in three steps. b) Before UV irradiation, the surface is hydrophilic with a CA of 6° . After irradiation, it becomes SHO with CA = 153° . c) TiO_2/PDMS could also be built on other substrates such as aluminum, and with other NPs including Al_2O_3 and SiO_2 , showing the versatility of present approach. d) The SHO heterostructure was put outdoor in open air to test its durability. CA is 155° after 276 d, indicating its high durability.

with various raw materials. We take $\text{TiO}_2/\text{PDMS}/\text{Cu}$ as an example. The fabrication process is shown schematically in **Figure 1a**. First, a PDMS layer was spin-coated onto Cu substrate and cured at 160°C for 10 min or at room temperature for a little longer time. Thickness of PDMS layer is $\approx 15\text{--}20\ \mu\text{m}$. Second, we dipped a droplet of TiO_2 -ethanol suspension on PDMS and then rolled it to fabricate an ultrathin oxide layer with a thickness of $\approx 1\ \mu\text{m}$. TiO_2 nanoparticles (NPs) with a mean diameter of $\approx 20\text{--}200\ \text{nm}$ are employed in the suspension. Finally we irradiated $\text{TiO}_2/\text{PDMS}/\text{Cu}$ under ultraviolet (UV) light for 2 min. UV irradiation from a 3 W light emitting diode (LED) flashlight is used with intensity of $10\ \text{mW cm}^{-2}$ at a distance of 2 cm away from $\text{TiO}_2/\text{PDMS}/\text{Cu}$. For comparison, femtosecond laser pulses with a power of $1.5 \times 10^{14}\ \text{mW cm}^{-2}$ are used by Vorobyev and Guo to create SHO metal surfaces.^[23] Besides, instruments such as laser and controlling system are not required in our method, and UV irradiation by LED is suitable for large-scale fabrication.

UV irradiation introduces a well-defined hydrophilicity-hydrophobicity transition on $\text{TiO}_2/\text{PDMS}/\text{Cu}$ heterostructure. Before irradiation, $\text{TiO}_2/\text{PDMS}/\text{Cu}$ is superhydrophilic with a CA of 6° (**Figure 1b**). Water spreads rapidly forming a flat film on such a surface. After irradiation, the surface becomes SHO with a CA of 153° . Water droplet slides down from the surface extremely quick, indicating its perfect water repellence (Movies S1 and S2, Supporting Information). In another test, a droplet slides down even though it is gently put on the horizontally placed surface, indicating a small roll-off angle ($<1^\circ$). Droplets with a diameter of 1.9 mm bounce multiple times (>17) when impacting the surface with velocities up to $1.98\ \text{m s}^{-1}$, with 70% kinetic energy conserved (Movie S3, Supporting Information). The bounce of droplet also reveals the surface is SHO.

A significant advantage in the present design of SHO heterostructure is its versatility. First, the choice of substrates is flexible. Metals such as Cu and Al, Si chips, glass, or plastics are all applicable without impairing superhydrophobicity (**Figure 1c** and **Figure S1**, Supporting Information). Second, a variety of NPs including TiO_2 , SiO_2 , Al_2O_3 , and carbon nanotubes all result in a SHO surface (**Figure 1c** and **Figure S2**, Supporting Information). Superhydrophobicity is independent of particle sizes whereas particles with a diameter ranging from 20 to 200 nm all show SHO features. Finally, a variety of simple treatments can achieve the hydrophilicity-hydrophobicity transition. Apart from UV irradiation, methods such as calcination at 300°C for 10 min and long-time storage are also practical (**Figures S3** and **S4**, Supporting Information).

When used in outdoor and other harsh environments, SHO surfaces should be stable and durable.^[9–12,18,22] We found that even heated at 350°C it remains SHO, confirming its robustness and thermal stability (**Figures S5** and **S6**, Supporting Information). We also placed the heterostructure outdoor in open air and measured CA at set intervals and the outdoor exposure includes the influence of rain falls in a way like artificial waterfall used by Jung and Bhushan.^[24] A straightforward test shows the contact angle is maintained at 153° after being put in flowing tap water (with an estimated velocity $2.08\ \text{m s}^{-1}$) for 3 h, indicating the excellent stability of the SHO coating.

Figure 1d shows the film remains SHO without apparent decay in CA even after more than 400 d, suggesting the heterostructure is of good durability. Here we consider a SHO surface maintaining its SHO property for over 365 d (a year) without artificial intervention as “long-lived.” For comparison, the CA of mechanically assembled SHO polymers decreases by $5^\circ\text{--}10^\circ$ within 7 d.^[9] The CA decrease of $\approx 10^\circ$ after outdoor exposure

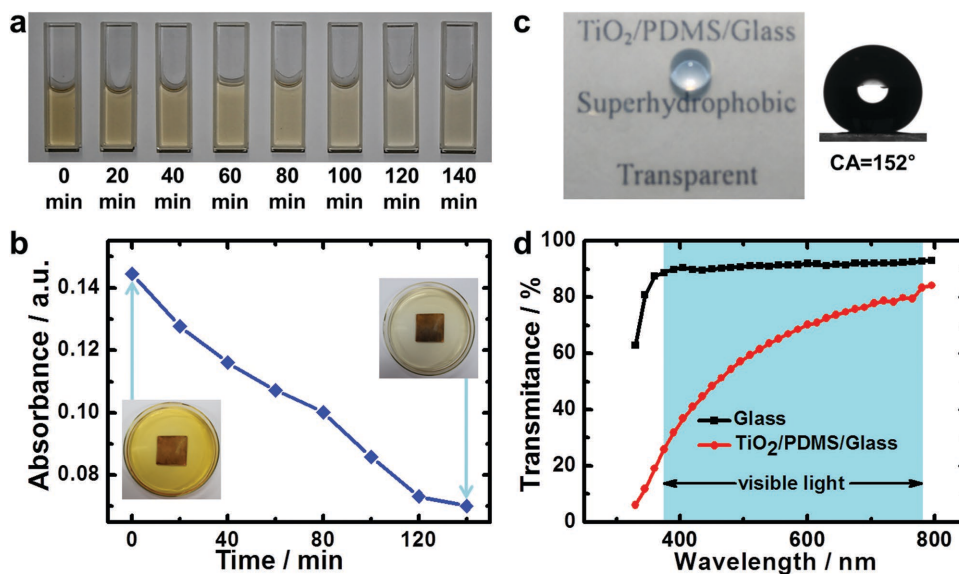


Figure 2. Photocatalysis and transparency of SHO heterostructure. a) Samples of methyl orange solution catalyzed by $\text{TiO}_2/\text{PDMS}/\text{Cu}$ at different times with color changing from yellow to colorless. b) Absorbance of methyl orange solution decreases from 0.145 to 0.07 a.u. during this process. c) TiO_2/PDMS becomes transparent when built on glass. Words behind the $\text{TiO}_2/\text{PDMS}/\text{Glass}$ can be clearly seen. CA of the heterostructure is 152° . d) Transmittance of the $\text{TiO}_2/\text{PDMS}/\text{Glass}$ sample. Wavelength range for visible light is marked by cyan area. The transmittance of $\text{TiO}_2/\text{PDMS}/\text{Glass}$ decreases by less than 28% compared to glass at wavelengths longer than 540 nm.

for 40 d and SHO properties of boehmite films maintained for 75 d are also reported.^[10,11] Long-term SHO is achieved for silicone nanofilament coatings upon a year of outdoor exposure, but the CA decreases and the sliding angle significantly increases after air exposure.^[12]

Functional SHO surfaces are even more challenging. With multifunctions SHO surfaces can enlarge their applications in fields of renewable energy and environmental engineering. For instance, photocatalytic SHO is an effective way to decompose organics and avoid oil-fouling, thus extending the lifetime of SHO surface.^[10,25–27] Curtain walls, automotive windshield and glasses require SHO surfaces with transparency.^[9–11,27] These functions are simultaneously achieved in our heterostructures. As shown in **Figure 2**, under UV irradiation methyl orange solution catalyzed by $\text{TiO}_2/\text{PDMS}/\text{Cu}$ changes from yellow to colorless with absorbance decreasing from initial 0.145 to 0.07 a.u. during 140 min. By mounting TiO_2/PDMS on glass we fabricated transparent heterostructures with CA of 152° (**Figure 2c**). Written words underneath the SHO film can be clearly seen. Measurements show that compared to glass, transmittance of the heterostructure decreases by less than 28% at wavelengths above 540 nm (**Figure 2d**).

To understand its outstanding SHO behavior, we characterize the $\text{TiO}_2/\text{PDMS}/\text{substrate}$ film microscopically. Atomic force microscopy and scanning electron microscopy (SEM) show that surface microstructures due to the presence of NPs contribute to superhydrophobicity and water repellence. From **Figure 3** and Table S1 of the Supporting Information we notice that TiO_2 film is >100 times rougher than PDMS before treatment. Root mean square (RMS) of the $3 \times 3 \mu\text{m}^2$ area TiO_2 film is 123 nm while RMS of the same area of PDMS is only 0.48 nm. We observe from the SEM image in **Figure 3c** that TiO_2 particles on the surface have an average diameter of ≈ 100 nm, which is responsible

for the measured roughness of 123 nm. **Figure 3d** indicates that the thickness of NPs layer ranges from 0.8 to 2.0 μm .

Self-supply of hydrophobic chemicals is key to the observed superhydrophobicity. We use Raman and infrared (IR) spectroscopy to detect chemical compositions on the surface. We find three characteristic bands of PDMS around 710, 689, and 491 cm^{-1} (marked by arrows) diminish after UV irradiation (**Figure 3e**).^[28] This suggests part of PDMS is decomposed. PDMS was reported to decompose under UV irradiation even in 3 min without photocatalysis.^[29] IR spectra in **Figure 3f** show absorptions around 1024 cm^{-1} and 1095 cm^{-1} increase sharply after UV irradiation. According to previous studies,^[30] silicides such as hexamethylcyclotrisiloxane (D3) and octamethylcyclotetrasiloxane (D4) show absorption peaks around 1024 and 1095 cm^{-1} . This observation suggests that some PDMS decomposes into silicides (D3 and D4) under UV irradiation with the assistance of the photocatalytic TiO_2 , which subsequently stick onto TiO_2 NPs and reach an equilibrium concentration (**Figure S9**, Supporting Information). X-ray photoelectron spectroscopy (XPS) analysis, which is sensitive to chemical composition at 0–10 nm under the surface, reveals the existence of silicides on TiO_2 surface (**Figure S10**, Supporting Information) and the atomic concentration of Si (C) is 12 (27) at% as listed in Table S2 of the Supporting Information. Surface tensions of these silicides are ≈ 19 mN m^{-1} at room temperature, leading to observed SHO properties when attached onto NPs, as schematically illustrated in **Figure 3g,h**. In the process of hydrophilicity-hydrophobicity transition, PDMS serves as a reservoir to supply low surface tension molecules to coat NPs and therefore the SHO heterostructure is endowed with self-supplying capacity. This mechanism is radically different from previously reported light-induced amphiphilic surfaces of TiO_2 ,^[31] or superhydrophobicity on TiO_2 nanotube arrays.^[32]

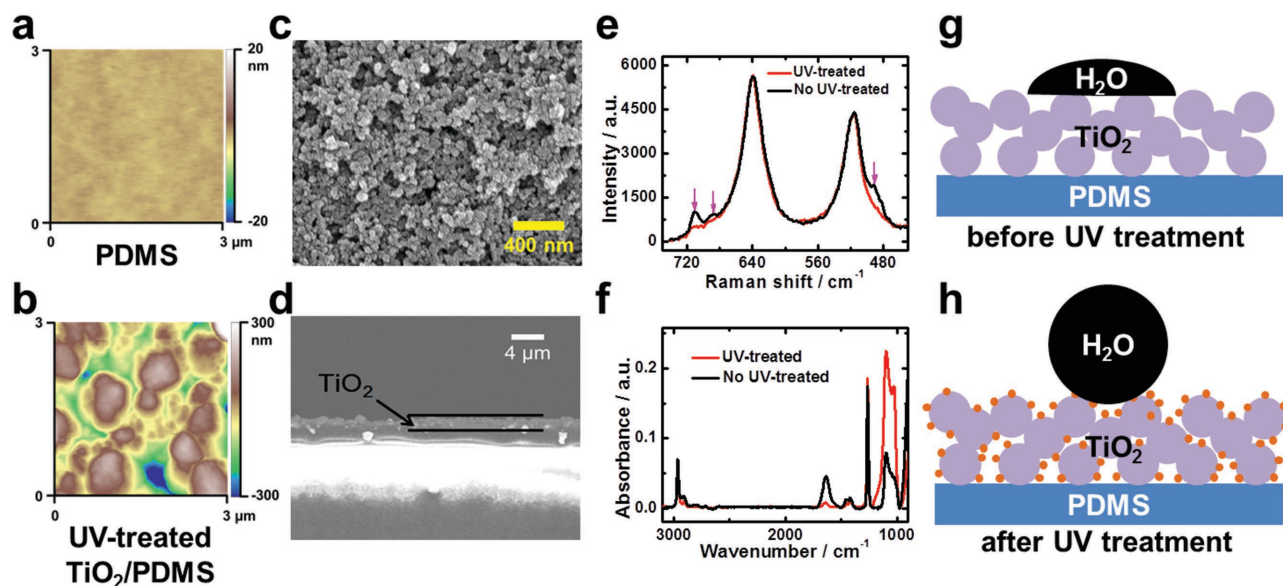


Figure 3. Characterization of microstructure and chemical composition. a) Atomic force microscopy (AFM) image on PDMS with an area $3 \times 3 \mu\text{m}^2$ showing it is smooth. b) AFM image of $3 \times 3 \mu\text{m}^2$ $\text{TiO}_2/\text{PDMS}/\text{Si}$, showing a rough surface. c) SEM image of TiO_2/PDMS surface showing the microstructure with particle sizes ≈ 100 nm. d) Side view image of the heterostructure revealing the thickness of TiO_2 film is in the range of 1–2 μm . e) Raman spectra indicate PDMS signals around 710, 689, and 488 cm^{-1} (indicated by arrows) of $\text{TiO}_2/\text{PDMS}/\text{Cu}$ diminish after UV treatment. f) IR spectra show that peaks around 1024 and 1095 cm^{-1} increase sharply in intensity. g, h) Cartoons illustrating the wettability transition induced by changes in surface structure and chemical composition. Decomposition products of PDMS after UV illumination (red dots) are self-supplied to cover TiO_2 NPs and to decrease surface tension.

The superhydrophilic-superhydrophobic transition caused by equilibrium small-molecule attaching onto TiO_2 NPs is also different from superhydrophobic $\text{TiO}_2\text{-SiO}_2@\text{PDMS}$ hybrid film produced by cumbersome sol-gel treatments.^[27,33] The biggest difference however lies in that the layered heterostructural design in the present work enables self-supply of coating agents

and effective sunlight shielding of PDMS by TiO_2 layer simultaneously, significantly extending the lifetime of superhydrophobicity. The self-supplying molecular coating thus represents a new mechanism to achieve SHO for a long duration.

Wettability pattern, composed of areas with contrasting wettabilities, has become critical in water collection, cell culture,

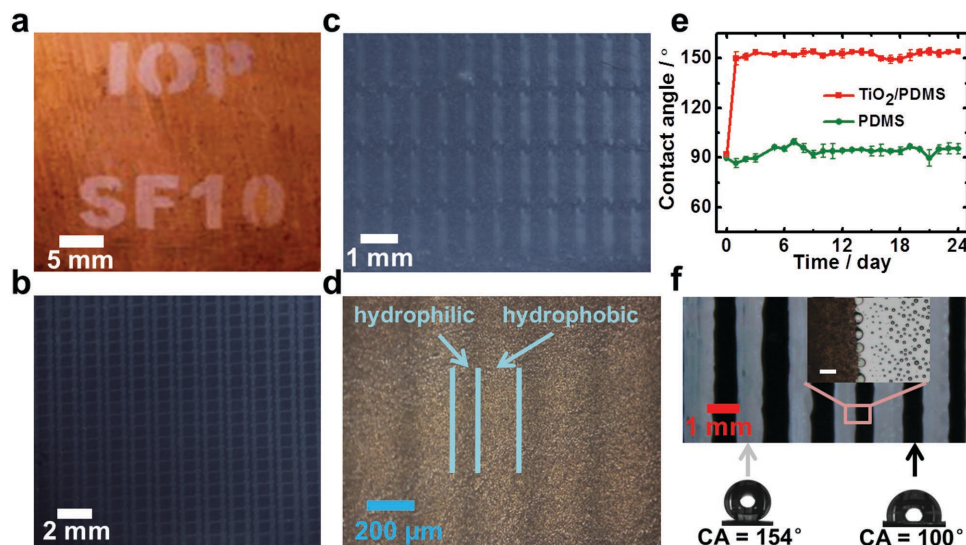


Figure 4. Various wettability patterns based on SHO heterostructure. a) The letters “IOP SF10” were written on the $\text{TiO}_2/\text{PDMS}/\text{Cu}$ surface by irradiating an optical mask with hollow letters, resulting in a visible contrast upon immersion in water. b, c) Microscale stripes containing hydrophilic and hydrophobic patterns on $\text{TiO}_2/\text{PDMS}/\text{Si}$. d) Microscale pattern denoted by water condensation. Water condenses into different shapes on areas with different wettability, resulting in visual contrast stripes. e) Contrast of CA on TiO_2/PDMS and PDMS. One day after rolling TiO_2 on treated PDMS, TiO_2 -covered PDMS (TiO_2/PDMS) becomes SHO while PDMS retains a CA of 90° . f) Wettability stripes by ink printing, with CA of 154° and 100° on neighboring stripes. Inset is water condensation on wettability patterns with scale bar of 100 μm .

transistors, and other applications.^[34–38] However, previous coating methods encounter difficulties in controlling fine wettability patterns. We demonstrate that our approach easily enables the fabrication of ultrafine wetting patterns. First, we irradiate the TiO₂/PDMS/Cu with UV below an optical mask (Figure S12, Supporting Information). The home-made optical mask contains patterns through which light can travel. The irradiated parts become SHO, while the surrounding parts remain hydrophilic. Figure 4a shows a wetting pattern written as “IOP SF10.” After immersion in water, regions on letters are SHO and keep dry, while other parts are wet, resulting a visibility contrast. Besides, this method can be used to fabricate micro-scale patterns as shown in Figure 4b–d. The size of pattern can be as small as tens to a 100 μm (Figure 4d). Second, we employ ink-printing approach using TiO₂ suspension as printing ink (Figure 4f) and the mechanism is illustrated in Figure 4e. After rolling TiO₂ suspension on PDMS, TiO₂-covered parts become SHO with CA over 150° while CA on bare PDMS remains 90°. With this method we can fabricate any patterns without limitations associated with optical masks. Interestingly, we find in moisture water condenses into large droplets on the boundary of areas with contrasting wettability, showing a promising potential for water collection (inset in Figure 4f).

3. Conclusion

In conclusion, we have developed a simple, rapid, and energy-saving approach to fabricate fluoride-free SHO heterostructures suitable for large-scale manufacturing, which does not involve any high-temperature calcination, intense laser ablation, or other energy-costly processes. The whole process requires as little as 2 min of UV irradiation, moderate heat treatment, or hours of storage. Ingredients needed in the heterostructures are only NPs (such as TiO₂) and PDMS, both of which are low cost and environment-friendly. Long durability and robustness against abrasion, heat, outdoor environments, and flowing tap water are demonstrated. Besides superhydrophobicity, multifunctions including photocatalysis and transparency are developed based on this heterostructural design. The film can be modulated to fabricate controllable wettability patterns by either light exposure or ink printing, favoring applications in water collection and nanobiotechnology.

Supporting Information

Supporting Information is available from the Wiley Online Library or from the author.

Acknowledgements

The authors acknowledge financial support from MOST (Grant Nos. 2012CB921403 and 2012CB933002), NSFC (Grant Nos. 11474328, 11290164, and 11222431), and the water project of CAS. The authors are grateful to Run Yang for IR measurements, Hao Wang for SEM characterization, and Wenbin Zhang for discussions on droplet bouncing on SHO surfaces.

Received: November 11, 2015

Revised: December 5, 2015

Published online:

- [1] S. Wang, L. Jiang, *Adv. Mater.* **2007**, *19*, 3423.
- [2] B. Bhushan, *Beilstein J. Nanotechnol.* **2011**, *2*, 66.
- [3] S. Singh, J. Houston, F. Swol, C. J. Brinker, *Nature* **2006**, *442*, 526.
- [4] A. W. Neumann, A. H. Abdelmssih, A. Hameed, *Int. J. Heat Mass Transfer* **1977**, *21*, 947.
- [5] H. Mertaniemi, V. Jokinen, L. Sainiemi, S. Franssila, A. Marmur, O. Ikkala, R. H. A. Ras, *Adv. Mater.* **2011**, *23*, 2911.
- [6] R. Tadmor, P. Bahadur, A. Leh, H. E. N'guessan, R. Jaini, L. Dang, *Phys. Rev. Lett.* **2009**, *103*, 266101.
- [7] A. Tropmann, L. Tanguy, P. Koltay, R. Zengerle, L. Riegger, *Langmuir* **2012**, *28*, 8292.
- [8] W. Barthlott, C. Neinhuis, *Planta* **1997**, *202*, 1.
- [9] J. Genzer, K. Efimenko, *Science* **2000**, *290*, 2130.
- [10] A. Nakajima, K. Hashimoto, T. Watanabe, K. Takai, G. Yamauchi, A. Fujishima, *Langmuir* **2000**, *16*, 7044.
- [11] M. Manca, A. Cannavale, L. D. Marco, A. S. Arico, R. Cingolani, G. Gigli, *Langmuir* **2009**, *25*, 6357.
- [12] J. Zimmermann, F. A. Reifler, U. Schrade, G. R. J. Artus, S. Seeger, *Colloids Surf., A* **2007**, *302*, 234.
- [13] A. B. D. Cassie, S. Baster, *Trans. Faraday Soc.* **1944**, *40*, 546.
- [14] P. Ball, *Nature* **1999**, *400*, 507.
- [15] J. Zhai, H. J. Li, Y. S. Li, S. H. Li, L. Jiang, *Physics* **2002**, *31*, 483.
- [16] T. Liu, C.-J. Kim, *Science* **2014**, *346*, 1096.
- [17] K. Lau, J. Bico, K. Teo, M. Chhowalla, G. Amaratunga, W. Milne, G. McKinley, K. Gleason, *Nano Lett.* **2003**, *3*, 1701.
- [18] X. Deng, L. Mammen, H.-J. Butt, D. Vollmer, *Science* **2012**, *335*, 67.
- [19] Y. Lee, Y. Yoo, J. Kim, S. Widhiarini, B. Park, H. C. Park, K. J. Yoon, D. Byun, *J. Bionic Eng.* **2009**, *6*, 365.
- [20] E. Martinez, K. Seunarine, H. Morgan, N. Gadegaard, C. Wilkinson, M. Riehle, *Nano Lett.* **2005**, *5*, 2097.
- [21] H. Wang, H. Zhou, A. Gestos, J. Fang, T. Lin, *ACS Appl. Mater. Interfaces* **2013**, *5*, 10221.
- [22] Y. Lu, S. Sathasivam, J. Song, C. R. Crick, C. J. Carmalt, I. P. Parkin, *Science* **2015**, *347*, 1132.
- [23] A. Y. Vorobyev, C. Guo, *J. Appl. Phys.* **2015**, *117*, 033103.
- [24] Y. Jung, B. Bhushan, *ACS Nano* **2009**, *3*, 4155.
- [25] T. Verho, C. Bower, P. Andrew, S. Franssila, O. Ikkala, R. Ras, *Adv. Mater.* **2011**, *23*, 673.
- [26] C. R. Crick, J. C. Bear, A. Kafzas, I. P. Parkin, *Adv. Mater.* **2012**, *24*, 3505.
- [27] C. Kapridaki, P. Maravelaki-Kalaitzaki, *Prog. Org. Coat.* **2013**, *76*, 400.
- [28] T. Park, S. Lee, G. H. Seong, J. Choo, E. K. Lee, Y. S. Kim, W. H. Ji, S. Y. Hwang, D.-G. Gweond, S. Lee, *Lab Chip* **2005**, *5*, 437.
- [29] B. Schnyder, T. Lippert, R. Kotz, A. Wokaun, V.-M. Graubner, O. Nuyken, *Surf. Sci.* **2003**, *532*, 1067.
- [30] M. J. Almond, R. Becerra, S. J. Bowes, J. P. Cannady, J. S. Ogden, R. Walsh, *Phys. Chem. Chem. Phys.* **2008**, *10*, 6856.
- [31] R. Wang, K. Hashimoto, A. Fujishima, M. Chikuni, E. Kojima, A. Kitamura, M. Shimohigoshi, T. Watanabe, *Nature* **1997**, *388*, 431.
- [32] S. Barthwal, Y. S. Kim, S. Lim, *J. Colloid Interface Sci.* **2013**, *400*, 123.
- [33] Z. Deng, W. Wang, L. Mao, C. Wang, S. Chen, *J. Mater. Chem. A* **2014**, *2*, 4178.
- [34] A. R. Parker, C. R. Lawrence, *Nature* **2001**, *414*, 33.
- [35] G. Piret, E. Galopin, Y. Coffinier, R. Boukherroub, D. Legrand, C. Slomianny, *Soft Matter* **2011**, *7*, 8642.
- [36] H. Siringhaus, T. Kawase, R. H. Friend, T. Shimoda, M. Inbasekaran, W. Wu, E. P. Woo, *Science* **2000**, *290*, 2123.
- [37] F. L. Geyer, E. Ueda, U. Liebel, N. Grau, P. A. Levkin, *Angew. Chem., Int. Ed.* **2011**, *50*, 8424.
- [38] A. Sidorenko, T. Krupenkin, A. Taylor, P. Fratzl, J. Aizenberg, *Science* **2007**, *315*, 487.